OBSERVATION OF THE INTERACTION OF PLASMONS WITH LONGITUDINAL OPTICAL PHONONS IN GaAs

A. Mooradian and G. B. Wright
Lincoln Laboratory,* Massachusetts Institute of Technology, Lexington, Massachusetts
(Received 2 May 1966)

We have observed the interaction of conduction-electron plasmons with the longitudinal optical (LO) phonon in the Raman spectrum of GaAs. As the carrier concentration of the samples is increased from $n = 2.3\times10^{15}$ cm^{-3} to $n = 2.9\times10^{18}$ cm^{-3}, the plasma frequency sweeps through the LO phonon frequency. When the plasma frequency approaches the phonon frequency, the LO phonon line observed in Raman-scattered light broadens and shifts to higher frequency (Fig. 1). A second small broad line at lower frequency appears and approaches the transverse optical (TO) phonon frequency as the carrier concentration increases. In the limit of high electron concentration, the LO phonon mode vibrates at the TO frequency, because the charge carriers have shielded out the polarization of the lattice vibrations. The TO phonon line is unaffected by carrier concentration. We believe that these results constitute a particularly clear experimental verification of the recently predicted[1-3] theoretical behavior of the plasmon-phonon system, as well as the first reported observation of Raman scattering by plasmons in solids.

Experimental.—The Raman-scattered light was generated in room temperature samples by a 1.0648-μ YAlG laser, operated cw at 1 W. It was observed at 90° with a Spex Model 1400 double monochromator and an S-1 photomultiplier. The gratings used were blazed at 0.75 μ. The fall-off of sensitivity toward longer wavelengths as a consequence of the combined spectral response of the S-1 photomultiplier and the 0.75-μ blazed gratings caused the anti-Stokes radiation to appear greater in intensity than the Stokes radiation. Ability to observe both Stokes and anti-Stokes radiation was a great help in discriminating against luminescence which sometimes occurred. The data in Fig. 1 are recorder traces which have been hand smoothed in some cases. Signal-to-noise ratios of the TO lines were in excess of 100 for the purest samples, and in excess of 20 in all cases. At the higher carrier concentrations used, the solubility limit of donors in GaAs is being approached, and we had some difficulty with sample inhomogeneity. The two points on the upper branch of the curve in Fig. 2 for the sample with $n = 1.7\times10^{18}$ cm^{-3} occurred for two runs where different portions of the sample were illuminated by the laser beam.

Discussion.—Varga[2] has shown that in the long-wavelength limit, the valence electrons, the polar lattice vibrations, and the conduction electrons make additive contributions to the total dielectric response function:

$$\epsilon_T(0,\omega) = \epsilon_\infty + \frac{\epsilon_0-\epsilon_\infty}{1-\omega^2/\omega_t^2} - \frac{\omega_p^2\epsilon_\infty}{\omega^2}, \qquad (1)$$

where $\omega_p^2 = 4\pi ne^2/m^*\epsilon_\infty$. For longitudinal waves, the eigenfrequencies of the system are given

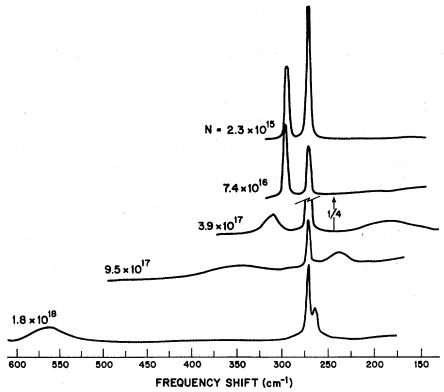

FIG. 1. The anti-Stokes Raman spectrum of n-type GaAs. The frequency-shift scale is not linear.

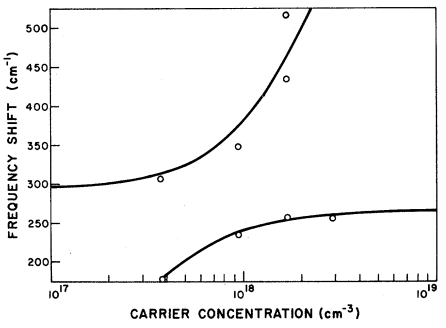

FIG. 2. The plasmon–LO-phonon interaction in GaAs. The solid lines are calculated from Eq. (2) for $\omega_t = 268$ cm^{-1}, $\omega_l = 291$ cm^{-1}, $\epsilon_\infty = 11.3$, $m^* = 0.07$.

by the zeros of the dielectric response,

$$x^2 = \tfrac{1}{2}\{\alpha + y^2 \pm [(\alpha + y^2)^2 - 4y^2]^{1/2}\}, \quad (2)$$

where we have written $x = \omega/\omega_t$, $y = \omega_p/\omega_t$, and $\alpha = \epsilon_0/\epsilon_\infty = \omega_l^2/\omega_t^2$. All of the constants in Eq. (1) are accessible to independent measurement, so the solid lines showing the eigenfrequencies in Fig. 2 contain no adjustable parameters. In the sample containing $n = 2.5\times10^{15}$ cm^{-3} carriers, where the interaction with carriers is negligible, we obtain $\omega_t = 268$ cm^{-1} and $\omega_l = 291$ cm^{-1} from the data of Fig. 1, and hence $\alpha = 1.179$. We take $m^* = 0.07$ and[4] $\epsilon_\infty = 11.3$ for the calculation of ω_p. The relative phonon content of the two coupled modes in Fig. 2 is of interest. Varga has defined a phonon strength $S_m = |\langle m|\varphi|0\rangle|^2$, where $\langle m|$ is the one-phonon function in the mth level, and φ is the phonon operator. He finds the interesting sum rule $\sum_m \omega_m S_m = \omega_l$. The phonon strength is given by

$$S_m = \frac{\alpha^{1/2}(\alpha-1)x_m^{\,3}}{(\alpha-1)x_m^{\,4} + y^2(1-x_m^{\,2})^2}. \quad (3)$$

We see from the curves of phonon strength in Fig. 3 that the Raman lines on the low-frequency side of the TO mode range in phonon strength from $S = 0.3$ for the $n = 3.8\times10^{17}$ cm^{-3} sample to $S = 1.05$ for $n = 3\times10^{18}$ cm^{-3}. The Raman lines on the high-frequency side of the TO mode have $S \simeq 1.0$ for $n = 2.5\times10^{15}$ cm^{-3} down to $S = 0.05$ for the line with the greatest frequency shift. This line may then be regarded as due to almost pure plasmon scattering.

The Raman cross section for scattering by phonons has been treated in third-order perturbation by Loudon,[5] and intraband contributions to the plasmon cross section have been calculated by McWhorter[6] and Platzman.[7] The importance of interband contributions to the plasmon cross section has been pointed out by Wolff.[8] While no theoretical treatment has been given for the cross section of the interacting plasmon-phonon system, the cross section for a given line should be proportional to the phonon or plasmon content of the mode at that frequency. Our ability to determine intensity and linewidth in the mixed-mode lines has been limited by the homogeneity of the samples presently available to us. The importance of inhomogeneity for line-breadth measurements will be proportional to the slope of the curves in Fig. 2, and the slope is greatest for modes with the greatest plasmon content. We see in Fig. 1 that the Raman lines with low-plasmon content are indeed narrower, as expected. Although absolute intensity measurements are difficult, an intrinsic property of the crystal, the TO mode intensity, serves as a good relative reference level. We have included in Fig. 1 the trace for one sample with $n = 7\times10^{16}$ cm^{-3} in which the intensity of the LO mode is greater than that of the TO mode, for both the Stokes and anti-Stokes spectrum. This feature was extremely concentration-dependent, and did not occur for adjacent slices of the same crystal. As the plasmon-phonon interaction is not strong at this concentration, the effect may be some type of resonant enhancement of the scattering cross section which depends critically upon ω_p.

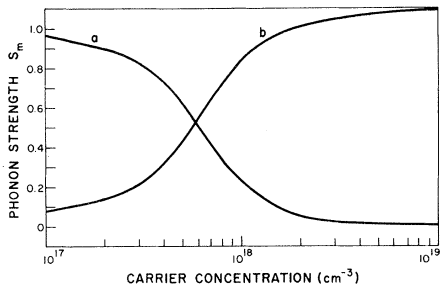

FIG. 3. The phonon strengths of the interacting plasmon–LO-phonon modes in GaAs. Curve (a) is for the high-frequency mode; curve (b) is for the low-frequency mode.

Conclusions.—We have observed Raman scattering by plasmons in GaAs, and the interaction of plasmons with the LO phonon mode. The frequency dependence of the interacting system fits the theoretical predictions. The intensity and linewidth dependence of the system as a function of plasma frequency remain to be studied in more homogeneous samples.

We gratefully acknowledge helpful discussions with A. L. McWhorter, who suggested the plasmon problem to us, and S. P. S. Porto, who provided much valuable information on the techniques of Raman spectroscopy. We particularly thank M. Bowden and C. F. Luck of Raytheon for the loan of the YAlG laser. We would also like to thank D. Wells for assistance with the measurements.

*Operated with support from the U. S. Air Force.

[1]Isaaki Yokota, J. Phys. Soc. Japan 16, 2075 (1961).

[2]B. B. Varga, Phys. Rev. 137, A1896 (1965). This reference contains references to earlier work in non-

degenerate systems.

[3]Y. C. Lee and N. Tzoar, Phys. Rev. 140, A396 (1965); K. S. Singwi and M. P. Tosi, to be published.

[4]D. T. F. Marple, J. Appl. Phys. 35, 1241 (1964).

[5]R. Loudon, Proc. Roy. Soc. (London) A275, 218 (1963).

[6]A. L. McWhorter, in Physics of Quantum Electronics, edited by P. L. Kelley, B. Lax, and P. E. Tannenwald (McGraw-Hill Book Company, New York, 1966), p. 111.

[7]P. M. Platzman, Phys. Rev. 139, A379 (1965).

[8]P. A. Wolff, Phys. Rev. Letters 16, 225 (1966).

TWO-BAND MODEL FOR BLOCH ELECTRONS IN CROSSED ELECTRIC AND MAGNETIC FIELDS

Wlodzimierz Zawadzki* and Benjamin Lax

National Magnet Laboratory,† Massachusetts Institute of Technology, Cambridge, Massachusetts

(Received 21 February 1966; revised manuscript received 10 May 1966)

The problem of Bloch electrons in the presence of external crossed magnetic and electric fields has recently become the subject of extensive investigations. Aronov[1] has calculated interband optical absorption in crossed fields using the one-band effective mass approximation (EMA). Peter and Hensel, Shindo, and Vrehen[2] have considered the case of degenerate bands using perturbation procedures, all based on the EMA. Recently Zak and Zawadzki,[3] using the Luttinger and Kohn treatment,[4] have shown that the validity of the one-band EMA is restricted to low values of the ratio E/H. Lax[5] indicated that to treat the problem for high values of E/H, one should start from a nonparabolic equation of relativistic type. This approach was applied by Praddaude[6] who showed that by taking into account the interaction between the two energy bands in question it is possible to obtain solutions with discrete eigenvalues for low E/H ratios and continuous eigenvalues for large E/H ratios. In this Letter we investigate this problem using essentially Kane's well-known procedure,[7] with emphasis on experimental consequences.

We calculate the matrix of the Hamiltonian for an electron in a periodic potential, with external magnetic and electric fields, in the Kohn-Luttinger representation $\chi_{nk}=\exp(i\vec{k}\cdot\vec{r})\times u_{n0}(\vec{r})$. After returning to the coordinate representation, the set of equations for envelope functions is obtained in the following form[8]:

$$\sum_{n'}[(\vec{P}^2/2m+e\vec{E}\cdot\vec{r}+\epsilon_n-\epsilon)\delta_{n'n}+\vec{P}\cdot\vec{\pi}_{n'n}]f_{n'}(\vec{r})=0. \quad (1)$$

Here $\vec{\pi}_{n'n}=(1/m)\langle u_{n'}|\vec{p}|u_n\rangle$ are determined by the interband matrix elements of momentum, ϵ_n is the energy at the bottom of the nth band (at $k=0$), $\vec{P}=\vec{p}+(e/c)\vec{A}$ is the kinetic momentum, and m is the free-electron mass. To simplify the problem we neglect the free-electron term in Eq. (1) [which is equivalent to neglecting the free mass in the effective-mass formula: $1/m_n^*=1/m+2\sum_{n'}|\pi_{nn'}|^2/(\epsilon_n-\epsilon_{n'})$], and consider only two spherical nondegenerate bands. Then the set of two equations can be solved by substitution. The tensor $(\vec{\pi}_{21}\vec{\pi}_{12})$ is symmetric and can be diagonalized. With the definition $1/m^*=2|\pi_{12}|^2/\epsilon_g$, choosing the gauge $\vec{A}=[-Hy,0,0]$, $\vec{E}=[0,E,0]$ in the diagonalizing coordinate system, we get

$$\left\{-\frac{\hbar^2}{2m^*}\frac{\partial^2}{\partial y^2}-\alpha y+\frac{m^*}{2}\left[\left(\frac{eH}{m^*c}\right)^2-\frac{2e^2E^2}{m^*\epsilon_g}\right]y^2+\frac{3}{4}\frac{\hbar^2}{2m^*}[y-(\epsilon_g+\epsilon)/eE]^{-2}\right\}\varphi(y)=\lambda\varphi(y), \quad (2)$$

where $\alpha=\hbar\omega_0k_x-eE(\epsilon_g+2\epsilon)/\epsilon_g$ with $\omega_c=eH/m^*c$ the effective cyclotron frequency, and $\lambda=\epsilon(\epsilon+\epsilon_g)/\epsilon_g-\hbar^2k_x^2/2m^*-\hbar^2k_z^2/2m^*$. The solution in terms of $\varphi(y)$ is

$$f_1=\exp[i(k_xx+k_zz)]\,|eEy-\epsilon_g-\epsilon|^{1/2}\varphi(y). \quad (3)$$

The last term on the left-hand side of Eq. (2) arises from the noncommutivity of the kinetic and potential energy and is equivalent to an effective spin-orbit coupling. A term of this type occurs also in the two-band model for deep impurity levels.[9] Without the "spin-orbit" term the eigenfunctions of Eq. (2) are given by the harmonic oscillator functions if $\omega_c^2-2e^2E^2/m^*\epsilon_g>0$ (with discrete eigenvalues easy to calculate in analytical form); if $\omega_c^2-2e^2E^2/m^*\epsilon_g=0$ and <0 they are given by the Airy functions and parabolic cylinder functions, respectively (with continuous spectra of eigenvalues). The spin-orbit term complicates the quantitative discussion of the equation, but qualitatively these conclusions remain essentially the same.